European Journal of Medicinal Chemistry 107 (2016) 1–11

Contents lists available at ScienceDirect

European Journal of Medicinal Chemistry

journal homepage: http://www.elsevier.com/locate/ejmech

Short communication

Discovery of a marine-derived bis-indole alkaloid fascaplysin, as a new class of potent P-glycoprotein inducer and establishment of its structure–activity relationship

Sudhakar Manda [a, b], Sadhana Sharma [c], Abubakar Wani [c], Prashant Joshi [a, b], Vikas Kumar [b, d], Santosh K. Guru [c], Sonali S. Bharate [d], Shashi Bhushan [b, c], Ram A. Vishwakarma [a, b], Ajay Kumar [c, **], Sandip B. Bharate [a, b, *]

[a] Medicinal Chemistry Division, CSIR-Indian Institute of Integrative Medicine, Canal Road, Jammu 180001, India
[b] Academy of Scientific & Innovative Research (AcSIR), CSIR-Indian Institute of Integrative Medicine, Canal Road, Jammu 180001, India
[c] Cancer Pharmacology Division, CSIR-Indian Institute of Integrative Medicine, Canal Road, Jammu 180001, India
[d] Preformulation Laboratory, PKPD Division, CSIR-Indian Institute of Integrative Medicine, Canal Road, Jammu 180001, India

ARTICLE INFO

Article history:
Received 14 August 2015
Received in revised form
10 October 2015
Accepted 28 October 2015
Available online 31 October 2015

Keywords:
Fascaplysin
β-carboline
P-glycoprotein induction
Acetylcholinesterase
Quaternary analogs
Alzheimer's disease

ABSTRACT

The screening of IIIM natural products repository for P-gp modulatory activity in P-gp over-expressing human adenocarcinoma LS-180 cells led to the identification of 7 natural products *viz.* withaferin, podophyllotoxin, 3-demethylcolchicine, agnuside, reserpine, seseberecine and fascaplysin as P-gp inducers. Fascaplysin (**6a**), a marine-derived bis-indole alkaloid, was the most potent among all of them, showing induction of P-gp with EC_{50} value of 25 nM. P-gp induction is one of the recently targeted strategy to increase amyloid-β clearance from Alzheimer brains. Thus, we pursued a medicinal chemistry of fascaplysin to establish its structure–activity relationship for P-gp induction activity. Four series of analogs *viz.* substituted quaternary fascaplysin analogs, D-ring opened quaternary analogs, D-ring opened non-quaternary analogs, and *β*-carbolinium analogs were synthesized and screened for P-gp induction activity. Among the total of 48 analogs screened, only quaternary nitrogen containing analogs **6a**–**g** and **10a**, **10h**–**l** displayed promising P-gp induction activity; whereas non-planar non-quaternary analogs **9a**–**m**, **13a**–**n**, **15a**–**h** were devoid of this activity. The P-gp induction activity of best compounds was then confirmed by western-blot analysis, which indicated that fascaplysin (**6a**) along with 4,5-difluoro analog of fascaplysin **6f** and D-ring opened analog **10j** displayed 4–8 fold increase in P-gp expression in LS-180 cells at 1 μM. Additionally, compounds **6a** and **6f** also showed inhibition of acetylcholinestease (AChE), an enzyme responsible for neuronal loss in Alzheimer's disease. Thus, fascaplysin and its analogs showing promising P-gp induction along with AChE inhibition at 1 μM, with good safety window (LS-180: IC_{50} > 10 μM, hGF: 4 μM), clearly indicates their promise for development as an anti-Alzheimer agent.

1. Introduction

Alzheimer's disease (AD) is the most common form of senile dementia and the fourth highest cause of disability and death in the elderly. It is characterized by the presence of three main brain hallmarks *viz.* diffuse neuronal loss with a particular involvement of the cholinergic system, extracellular protein deposits (amyloid-β plaques) and intracellular protein deposits (neurofibrillary tangles, NFTs) [1–3]. All current therapies are based on the cholinergic hypothesis and demonstrate only symptomatic treatment. P-glycoprotein (P-gp) is highly expressed on the luminal surface of brain capillary endothelial cells and contributes to the BBB. The recent two independent clinical studies [4,5] observed that AD patients have decreased clearance of CNS amyloid-β compared to healthy volunteers. The rate of Aβ production is same as that in healthy volunteers; whereas rate of clearance is impaired by 25–30%. High levels of Aβ then initiates cascade of events

* Corresponding author. Medicinal Chemistry Division, CSIR-Indian Institute of Integrative Medicine, Canal Road, Jammu 180001, India.
** Corresponding author.
E-mail addresses: ajaykmahajan@hotmail.com (A. Kumar), sbharate@iiim.ac.in (S.B. Bharate).

http://dx.doi.org/10.1016/j.ejmech.2015.10.049
0223-5234/

culminating in neuronal damage and death manifesting as progressive dementia of the AD type. There is a direct link between P-gp and Aβ metabolism in vivo and the P-gp activity at the BBB could affect risk for developing AD as well as provide a novel diagnostic and therapeutic target [6]. Thus, it is evident that drugs that have ability to increase levels of P-gp should increase amyloid-β clearance. Large number of plant extracts and their natural products have been reported to possess potent P-gp induction activity, including rifampicin, St. John's Wort (*Hypericum perforatum*) extract and its constituent hyperforin (**1**) [7–11]. Similarly, the prenylated phloroglucinol colupulone (**2**) isolated from Hops extract is a potent activator of PXR (a nuclear receptor of P-gp) [12]. Recently oleocanthal (**3**) [13] has been reported to increase Aβ-transport across BBB *via* P-gp induction. Our group also demonstrated that P-gp inducers (colupulone analog **4** [14] and quinoline **5** [15]) modulates Aβ-transport. Thus, it is clear that natural products are potential source for identification of P-gp inducer leads for AD drug development *via* amyloid-β clearance strategy.

In continuation to our efforts in the area of discovery of P-gp modulators from natural products [14–17], herein we report discovery of fascaplysin (**6a**), a marine-derived bisindole alkaloid, as a new class of P-gp inducers. The P-gp induction activity of fascaplysin was discovered while screening in-house natural products repository for P-gp modulation activity.

Fascaplysin (**6a**) is a fused benzoyl-linked β-carbolinium alkaloid isolated from marine sponge *Fascaplysinopsis* Bergquist sp. collected in the South Pacific near the Fiji Island as an unusual antimicrobial pigment [18]. It is reported to possess cytotoxicity in mouse leukemia L-1210 cells and cervical cancer HeLa cells [19], a Cdk-4 specific inhibitory activity (IC_{50} 0.35 μM) [20–22], and acetylcholinesterase (AChE) inhibitory activity [23]. Herein, we report its P-gp induction activity, and preliminary structure–activity relationship, along with its AChE inhibition activity. The chemical structures of compounds **1**–**6** are shown in Fig. 1.

2. Results and discussion

2.1. Screening of IIIM compound repository for P-gp induction activity

The in-house natural products repository (302 natural products) was screened for P-gp induction activity in P-gp overexpressing human adenocarcinoma LS-180 cells using rhodamine 123 (Rh123) cell exclusion method and rifampicin (10 μM) was used as a positive control. The test concentration of 5 μM was used for preliminary screening. This concentration was selected in order to avoid chance of missing any possible P-gp inducer in the first step. This screening resulted in identification of 7 natural products as promising P-gp inducers *viz*. withaferin, podophyllotoxin, 3-demethylcolchicine, agnuside, reserpine, sesibiricin and fascaplysin. The P-gp induction activity and structures of these 7 hits are shown in Fig. 2.

2.2. Synthesis of fascaplysin and its analogs to establish structure–activity relationship

A series of quaternary fascaplysin analogs (series 1) were synthesized using our recently reported two-step strategy [23] as depicted in Scheme 1. Tryptamine (**7**) was treated with 2-chloro substituted phenyl glyoxals **8a**–**m** in presence of Pd/C in acetic acid which produced β-carbolines **9a**–**m** (Schemes 1 and 2). β-Carbolines **9a**–**g** on heating at 220 °C for 20 min resulted in ring closure to produce fascaplysin (**6a**) and its analogs **6b**–**g** in 70–80% yield (Scheme 1).

Next, we synthesized D-ring opened fascaplysin analogs (series 2) with keeping quaternary nitrogen intact using the protocol shown in Scheme 2. β-Carbolines **9a** and **9h**–**m** on treatment with methyl iodide gave quaternary salts **10a** and **10h**–**l** in 60–65% yield (Scheme 2). D-ring opened non-quaternary analogs **9a**–**m** (series 3), prepared in Schemes 1 and 2, were also used for P-gp screening.

Further, a series of β-carboline based non-planar analogs (series 4) of fascaplysin were synthesized starting from commercially available tetrahydro-β-carboline (**11**). Reaction of tetrahydro-β-carboline (**11**) with different acyl halides **12a**–**n** in CH_2Cl_2 in presence of sodium hydroxide produced *N*-acyl β-carbolines **13a**–**n** in 63–82% yield (Scheme 3). Similarly a series of N-alkylated *β*-carbolines **15a**–**h** were synthesized by treatment of tetrahydro-*β*-carboline (**11**) with different heterocycle linked alkyl halides **14a**–**h** as depicted in Scheme 3 [24].

2.3. P-gp induction activity

All synthesized compounds from all four series (total 48

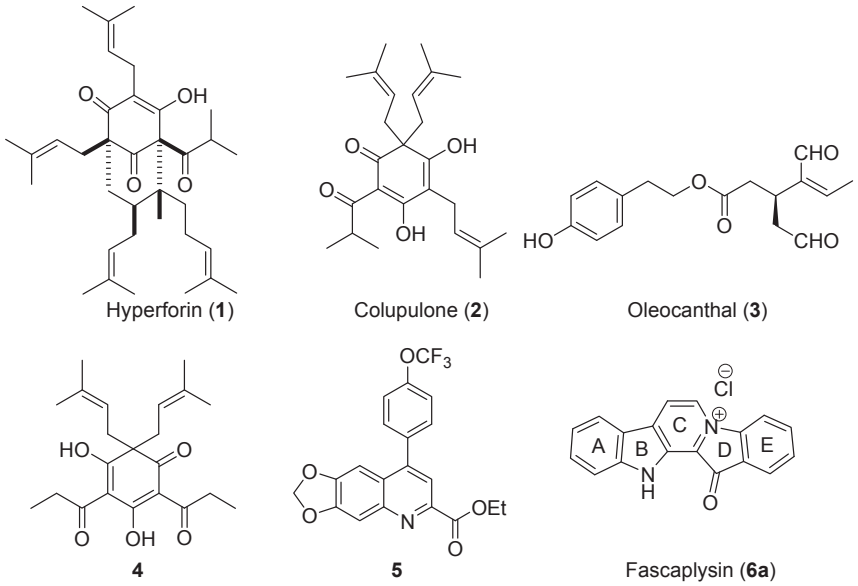

Fig. 1. Structures of P-gp inducer natural products **1**–**3**, our P-gp inducer leads **4**–**5**, and bis-indole alkaloid fascaplysin (**6a**).

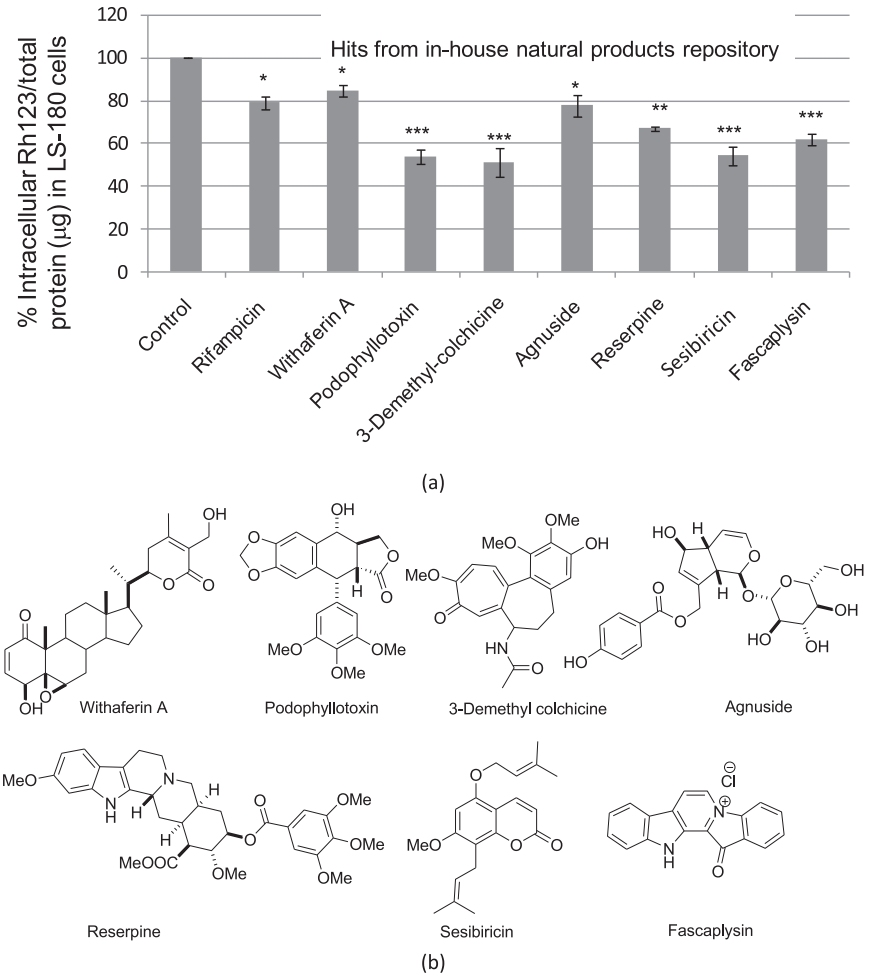

Fig. 2. P-gp induction activity (a) and structures (b) of natural product hits identified from screening of institutional natural product repository in LS-180 cells (Rifampicin was used as a positive control; the test concentration of 10 μM was used for rifampicin and 5 μM for all test compounds). The statistical comparisons were made between control *versus* compounds. The p value <0.5 was considered to be significant. P value *<0.5, **<0.01, ***<0.001, ns no significance.

compounds) were screened for P-gp induction activity in P-gp overexpressing adenocarcinoma LS180 cells at 1 μM. The decrease in the % intracellular accumulation (compared to control) of Rh123 indicates induction of P-gp. Rifampicin (10 μM) was used as a reference P-gp inducer. Statistical comparisons were made between control *versus* compounds by using Bonferroni test. Fascaplysin (**6a**) was found to display P-gp induction activity at 1 μM, as indicated by decreased intracellular accumulation of Rh123 levels up to 57% in LS180 cells.

Several fascaplysin analogs showed ability to induce p-glycoprotein as shown in Table 1. The obtained P-gp screening results revealed important structure–activity relationship features. All quaternary nitrogen containing analogs **6a**–**g** (series 1), **10a** and **10h**–**l** (series 2) showed promising P-gp induction activity. However, the D-ring opened analogs without quaternary nitrogen **9a**–**m** (series 3) were inactive. The tetrahydro β-carboline analogs (non-planar, non-quaternary) **13a**–**n** and **15a**–**h** (series 4) were also devoid of P-gp induction activity at 1 and 5 μM. Thus, it is evident that, upon opening of the D-ring of fascaplysin while maintaining C-ring nitrogen in quaternary form (analog **10a**, **10h**–**l**), the P-gp induction activity was maintained. However, on removal of quaternary status of the C-ring nitrogen, the P-gp induction activity was completely diminished. This indicates that, the opening of D-ring is tolerated; as far as the quaternary status of C-ring nitrogen is maintained.

As shown in Table 1, fascaplysin (**6a**) and its analogs **6f** and **10j** showed reduced % intracellular rhodamine-123 levels (57%, 49% and 70%, respectively), in comparison to untreated control cells (100%), indicating their effect as a P-gp inducer. The effect of these key compounds was also checked at lower concentrations. As shown in Table 2, these compounds showed significant decrease in the intracellular Rh123 levels at very low concentration, 62.5 nM. The EC_{50} of fascaplysin was determined and was found to be 25 nM.

The promising p-glycoprotein induction activity of these compounds was further confirmed by western-blot analysis at 1 μM. Upon exposure to compounds **6a**, **6f** and **10j**, the P-glycoprotein expression was found to be significantly increased (by 4–8 fold) (Fig. 3).

All compounds were tested for in-vitro cytotoxicity in LS-180 cells using MTT assay at 10 μM and 48 h treatment time, wherein most of the compounds showed >50% cell viability (IC_{50} > 10 μM) (Table 1). Furthermore, the best compound fascaplysin (**6a**) was also screened for cytotoxicity in normal human gingival fibroblast hGF cells. It showed cytotoxicity in this cell line with IC_{50} value of 4 μM. These cytotoxicity results indicated that there is a good therapeutic index of these compounds for P-gp induction.

2.4. AChE inhibition activity

Recently, fascaplysin (**6a**) was reported as AChE inhibitor [23].

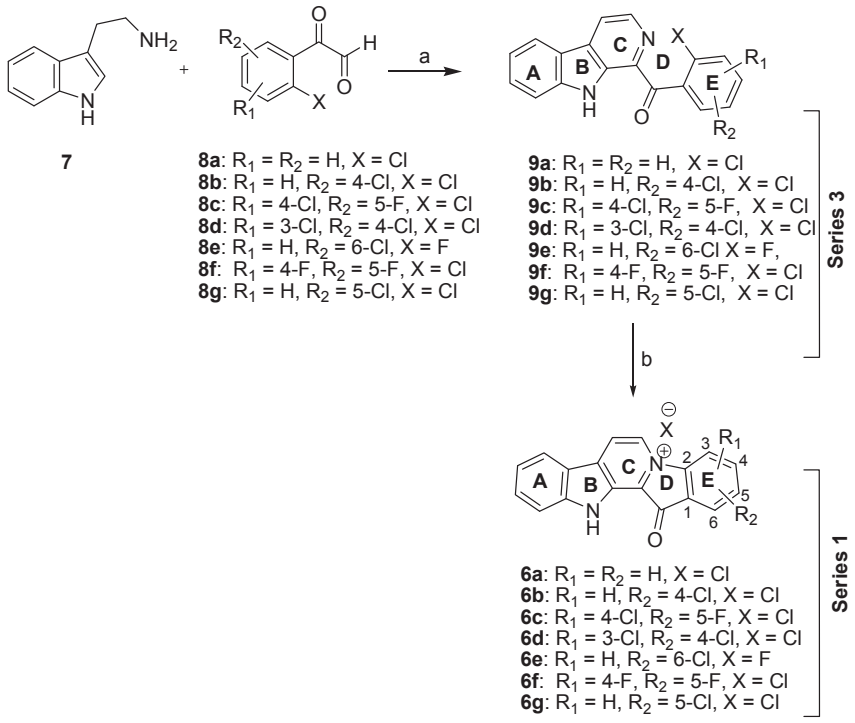

Scheme 1. Synthesis of fascaplysin and its quaternary analogs **6a**–**g**. Reagents and conditions: (a). 10% Pd/C, AcOH, reflux, 3 h, 65–85%; (b). 220 °C, 20 min, 70–80%.

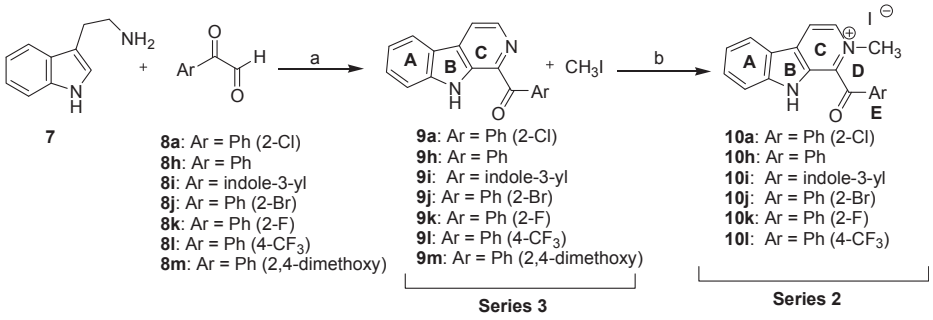

Scheme 2. Synthesis of D-ring opened analogs of fascaplysin **10a**, **10h**–**l**. Reagents and conditions: (a). 10% Pd/C, AcOH, reflux, 3 h, 65–85%; (b). ACN, 80 °C, 12 h, 60–75%.

Based on this report, in addition to their P-gp induction activity, we screened best identified P-gp inducers **6f** and **10j** for AChE inhibition activity at the concentration (1 μM) at which P-gp induction activity was performed. Compound **6f** showed 62% inhibition of AChE at 1 μM; whereas compound **10j** showed only 7% inhibition of AChE at this concentration.

In accordance to the recent literature precedence and the availability of human AChE crystal structure, best compound **6f** which exhibited significant P-gp efflux function induction as well as AChE inhibition, was further studied for its interaction with human AChE (PDB ID: 4EY7). In previous publication [23], we have reported that parent compound fascaplysin (**6a**) bounds only at the peripheral anionic site by interacting with the Trp-286 residue and does not interacts directly with the catalytic site residue Trp-86 (as shown in Section S3 of supporting information). Similar to fascaplysin, the analog **6f** also interacts only with the peripheral anionic site residue Trp-286 (corresponding residue in human AChE) by hydrophobic π−π interactions. But, in addition to the hydrophobic interactions, it enters deeper into the catalytic pocket due to the additional bulkier halogen groups on the E-ring, and exhibits polar H-bonding with the Gly-221 and H_2O 737 at AChE catalytic site, as shown in Fig. 4; and thereby it prevents the entry of substrate ACh to the catalytic site.

2.5. Aqueous solubility of best compounds

The solubility of most potent compounds **6a**, **6f**, and **10j** was determined in water, PBS, SGF, and SIF. Fascaplysin (**6a**) showed high solubility in water as well as biological fluids PBS, SGF, and SIF (>1500 μg/ml). Compound **6f** showed high solubility in water (>1500 μg/ml), moderate solubility in PBS and SGF, however less solubility in SIF (<5 μg/ml). Compound **10j** also showed high solubility in water as well as biological fluids PBS, SGF, and SIF (800 μg/ml). Solubility results are shown in Table 3.

3. Conclusion

In summary, from the screening of in-house natural products repository for P-gp induction activity, we have identified fascaplysin as a new class of P-gp inducer. A medicinal chemistry of

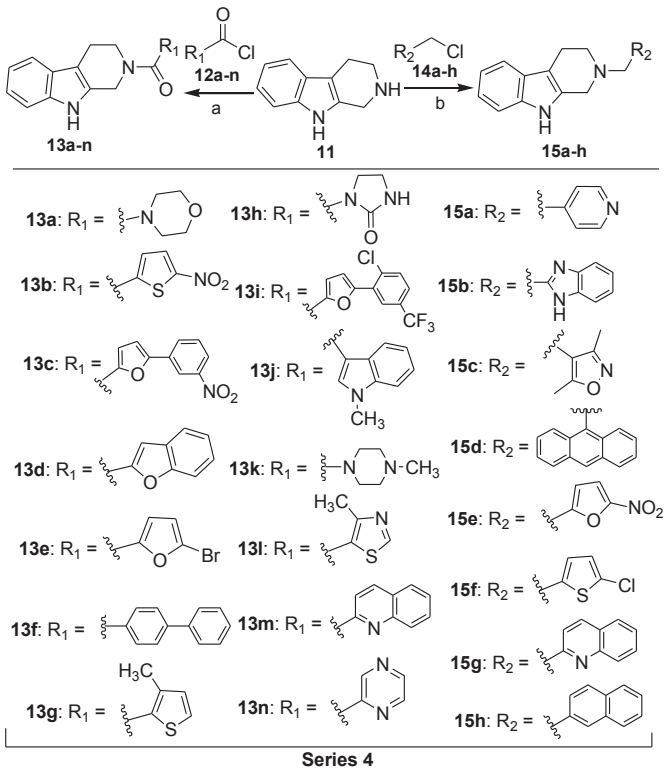

Scheme 3. Synthesis of non-planar and non-quaternary analogs of fascaplysin **13a**–**n** and **15a**–**h**. Reagents and conditions: (a) CH_2Cl_2, NaOH, 0 °C, 15 min then rt, 3 h, 63–82%; (b) K_2CO_3, CH_3CN, 3 h, rt, 66–78%.

fascaplysin led to the establishment of SAR of this scaffold and identified analog **10j** which showed 8-fold increase in P-gp expression in LS-180 cells, indicating its promise to enhance Aβ clearance from AD brains. Furthermore, compounds **6a**, **6f** and **10j** showed good solubility in water as well as simulated body fluids. Thus, results presented in this work, indicates promise of this scaffold for development as an anti-Alzheimer agent.

4. Experimental section

4.1. General

All chemicals were obtained from Sigma–Aldrich Company and used as received. ^{1}H, ^{13}C and DEPT NMR spectra were recorded on Brucker-Avance DPX FT-NMR 500 and 400 MHz instruments. Chemical data for protons are reported in parts per million (ppm) downfield from tetramethylsilane and are referenced to the residual proton in the NMR solvent ($CDCl_3$, 7.26 ppm; CD_3OD, 3.31 ppm). Carbon nuclear magnetic resonance spectra (^{13}C NMR) were recorded at 125 MHz or 100 MHz: chemical data for carbons are reported in parts per million (ppm, δ scale) downfield from tetramethylsilane and are referenced to the carbon resonance of the solvent ($CDCl_3$, 77.16 ppm; CD_3OD, 49.0). ESI-MS and HRMS spectra were recorded on Agilent 1100 LC-Q-TOF and HRMS-6540-UHD machines. IR spectra were recorded on Perkin–Elmer IR spectrophotometer. Melting points were recorded on digital melting point apparatus. HPLC analysis was done on Shimadzu HPLC system (model: LC-6AD) equipped with a PDA detector (model: SPD-M20A) using Inertsil C_8 (3.5 μ, 4.6 × 250 mm) column using ACN: water (50: 50) mobile phase by isocratic elution at flow rate of 1 ml/min.

4.2. Synthesis of substituted phenyl glyoxals **8a**–**m**

The solution of SeO_2 (12.79 mmol) in 1,4-dioxane/water (10 mL, 95: 5) was heated at 60 °C for 3 h. Substituted acetophenones (12.98 mmol) were added and the reaction mixture was refluxed for 4 h. Reaction mixture was filtered and the filtrate was concentrated. The formation of glyoxal was confirmed by TLC and MS. The crude products **8a**–**m** (>85% pure) were directly used for the next step without purification [25].

4.3. General procedure for preparation of β-carbolines **9a**–**m**

To the solution of tryptamine (7, 6.25 mmol) and substituted phenyl glyoxals **8a**–**m** (7.5 mmol) in glacial acetic acid (15 mL) was added 10% Pd/C catalyst (20 mol%) and reaction mixture was refluxed for 3 h. The reaction mixture was filtered through celite and the filtrate was concentrated on rotary evaporator to get crude product which on silica gel column chromatography (20% ethyl acetate/hexane) gave corresponding β-carbolines **9a**–**m** in 65–85% yield.

4.3.1. 2-Chlorophenyl(9H-pyrido[3,4-b]indol-1-yl)methanone (**9a**)

Yellow solid; yield: 85%; m.p. 203–205 °C; HPLC: >99% (t_R = 16.71 min); ^{1}H NMR (500 MHz $CDCl_3$, ppm): δ 10.42 (brs, NH, 1H), 8.56 (d, J = 4.8 Hz, 1H), 8.20–8.15 (m, 2H), 7.66–7.59 (m, 3H), 7.53–7.35 (m, 4H); ^{13}C NMR (100 MHz, $CDCl_3$, ppm): δ 197.57, 141.25, 138.78, 138.39, 136.80, 135.46, 132.77, 132.06, 131.88, 131.83, 131.16, 130.01, 129.90, 126.48, 121.89, 120.70, 119.16, 112.10; IR ($CHCl_3$): ν_{max} 3421, 3058, 2360, 2340, 2360, 1699, 1646, 1626, 1592, 1430, 1212 cm^{-1}; ESI-MS: m/z 307.06 $[M+H]^+$; HR-ESIMS: m/z 307.0619 calcd for $C_{18}H_{12}ClN_2O + H^+$ (307.0632).

4.3.2. (2,4-Dichlorophenyl)(9H-pyrido[3,4-b]indol-1-yl)methanone (**9b**)

Yellow solid; yield: 68%; m.p. 212–215 °C; HPLC: >99% (t_R = 25.90 min); ^{1}H NMR (400 MHz, $CDCl_3$, ppm): δ 10.39 (s, NH, 1H), 8.55 (d, J = 4.0 Hz, 1H), 8.20–8.17 (m, 2H), 7.65–7.53 (m, 4H), 7.42–7.38 (m, 2H); ^{13}C NMR (100 MHz, $CDCl_3$, ppm): δ 196.42, 141.27, 138.82, 136.89, 136.73, 136.70, 135.20, 133.19, 132.99, 132.03, 129.62, 127.04, 126.75, 121.97, 121.16, 120.73, 119.36, 112.12; IR ($CHCl_3$): ν_{max} 3433, 3368, 3061, 2923, 2851, 1899, 1653, 1625, 1555, 1493, 1463, 1429, 1373, 1282, 1259, 1245, 1149, 1118, 1095, 1064, 1050, 1013 cm^{-1}; ESI-MS: m/z 341.02 $[M+H]^+$; HR-ESIMS: m/z 341.0221 calcd for $C_{18}H_{11}Cl_2N_2O + H^+$ (341.0242).

4.3.3. (2,4-Dichloro-5-fluorophenyl)(9H-pyrido[3,4-b]indol-1 yl) methanone (**9c**)

Yellow solid; yield: 65%; m.p. 209–211 °C; HPLC: >99% (t_R = 29.26 min); ^{1}H NMR (400 MHz, $CDCl_3$, ppm): δ 10.39 (s, NH, 1H), 8.54 (d, J = 8.0 Hz, 1H), 8.17–8.15 (m, 2H), 7.63–7.51 (m, 3H), 7.42–7.36 (m, 2H); ^{19}F NMR (376.5 Hz, $CDCl_3$, ppm): δ −116.99 to −117.03 (m, 1F); ^{13}C NMR (100 MHz, $CDCl_3$, ppm): δ 194.92, 156.36 ($^1J_{CF}$ = 150.51 Hz), 141.24, 138.88, 136.92, 134.68, 132.09, 131.66, 129.69, 127.43, 123.73, 121.98, 121.25, 120.65, 119.58, 118.21, 117.91, 112.13; IR ($CHCl_3$): ν_{max} 3368, 2920, 2850, 2343, 1653, 1625, 1596, 1572, 1493, 1462, 1430, 1391, 1315, 1282, 1256, 1204, 1174, 1149, 1118, 1090, 1062, 1017 cm^{-1}; ESI-MS: m/z 359.01 $[M+H]^+$; HR-ESIMS: m/z 359.0145 calcd for $C_{18}H_{10}Cl_2FN_2O + H^+$ (359.0148).

4.3.4. (2,3,4-Trichlorophenyl)(9H-pyrido[3,4-b]indol-1-yl) methanone (**9d**)

Yellow solid; yield: 75%; m.p. 216–218 °C; HPLC: 91% (t_R = 17.73 min); ^{1}H NMR (400 MHz, $CDCl_3$, ppm): δ 10.34 (s, NH, 1H), 8.53 (t, J = 3.6 Hz, 1H), 8.18 (t, J = 7.2 Hz, 2H), 7.65–7.53 (m, 3H), 7.41–7.38 (m, 2H); ^{13}C NMR (100 MHz, $CDCl_3$, ppm): δ 195.84,

Table 1
In-vitro P-gp induction and cytotoxic activity of fascaplysin and its analogs in LS-180 cells.[a]

Entry	% Rh123 accumulation in LS-180 cells at 1 μM after 48 h[b,c]	% viability of LS-180 cells at 10 μM[c]
Control	100	100
Rifampicin	67.1 ± 4.6***	nd
6a	57.58 ± 4.7***	57.5 ± 3.7
6b	57.1 ± 9.2***	66.2 ± 8.1
6c	55.5 ± 6.9***	36.8 ± 6.8
6d	57.8 ± 8.3***	57.4 ± 8.4
6e	59.2 ± 6.7***	63.4 ± 10.2
6f	49.6 ± 1.2***	63.5 ± 3.6
6g	58.7 ± 7.8***	67.9 ± 6.9
10a	71.4 ± 8.4**	69.7 ± 9.0
10h	75.2 ± 9.1**	77.5 ± 0.3
10i	77.6 ± 7.6**	69.1 ± 9.4
10j	70.1 ± 6.7**	69.1 ± 5.9
10k	79.0 ± 6.0**	69.8 ± 7.1
10l	78.5 ± 5.8**	75.7 ± 4.9
9a	105.4 ± 4.4ns	89.4 ± 7.6
9b	97.3 ± 0.2ns	98.8 ± 4.0
9c	106.1 ± 0.5ns	92.4 ± 8.6
9d	104.1 ± 1.1ns	84.9 ± 9.3
9e	89.6 ± 4.1***	60.1 ± 1.4
9f	112.4 ± 5.3**	81.9 ± 5.6
9g	102.7 ± 3.4ns	69.6 ± 7.8
9h	94.6 ± 2.6ns	67.5 ± 4.6
9i	99.4 ± 1.4ns	78.7 ± 3.8
9j	104.8 ± 1.8ns	80.3 ± 2.8
9k	100.9 ± 4.1ns	98.4 ± 3.9
9l	106.6 ± 1.8ns	105.6 ± 2.6
9m	107.8 ± 4.1ns	82.2 ± 2.7

nd: not determined.
[a] All series 4 compounds **13a**–**n** and **15a**–**h** were devoid of P-gp induction activity at 5 μM.
[b] P-gp induction activity of compounds was checked at 1 μM; and was measured in terms of the % intracellular accumulation of rhodamine 123/total protein (μg) inside LS-180 cells. The decrease in % intracellular accumulation (compared to control) of Rh123 indicates induction of P-gp. Rifampicin (10 μM) was used as a reference P-gp inducer. The statistical comparisons were made between control *versus* compounds. The p value <0.5 was considered to be significant. P value*< 0.5,**<0.01,***<0.001, ns no significance.
[c] Values are shown as average of three experiments ± SD.

Table 2
The percentage intracellular Rh123 levels in LS-180 cells after treatment with compounds **6a**, **6f** and **10j** at nanomolar concentrations.

Compound, nM	% intracellular Rh123 levels in LS-180 cells[a]		
	6a	**6f**	**10j**
0	100	100	100
62.5	42.89 ± 1.61	35.54 ± 0.77	80.02 ± 7.03
125	39.28 ± 5.41	33.79 ± 3.73	41.78 ± 0.91
250	43.71 ± 4.01	35.29 ± 3.50	42.34 ± 7.23
500	34.54 ± 0.21	30.62 ± 2.85	33.65 ± 2.89

[a] Values are shown as average of three experiments ± SD.

141.22, 138.95, 138.71, 136.89, 135.76, 134.77, 132.67, 132.07, 129.71, 128.21, 127.38, 122.01, 121.25, 120.67, 119.58, 112.13; IR ($CHCl_3$): ν_{max} 3467, 3431, 3094, 2925, 2853, 2350, 2071, 1930, 1915, 1656, 1637, 1625, 1573, 1492, 1464, 1429, 1361, 1325, 1314, 1282, 1254, 1214, 1197, 1148, 1107, 1064 cm^{-1}; ESI-MS: *m/z* 374.80 $[M+H]^+$; HR-ESIMS: *m/z* 374.9865 calcd for $C_{18}H_{10}Cl_3N_2O + H^+$ (374.9853).

*4.3.5. (2-Chloro-6-fluorophenyl)(9H-pyrido[3,4-b]indol-1-yl) methanone (**9e**)*

Yellow solid; yield: 76%; m.p. 218–220 °C; HPLC: 91% (t_R = 10.64 min); ^1H NMR (400 MHz, $CDCl_3$, ppm): δ 10.31 (s, NH, 1H), 8.47 (d, *J* = 4.0 Hz, 1H), 8.11 (t, *J* = 4.0 Hz, 2H), 7.58–7.56 (m, 2H), 7.36–7.25 (m, 3H), 7.09–7.05 (m, 1H); ^{19}F NMR (376.5 Hz, $CDCl_3$, ppm): δ −111.98 to −112.02 (m, 1F); ^{13}C NMR (100 MHz, $CDCl_3$, ppm): δ 192.38, 157.70 ($^1J_{CF}$ = 248.5 Hz), 139.23, 137.23, 134.48, 133.31, 129.93, 129.31, 127.60, 125.81, 125.64, 123.52, 119.99, 119.18, 118.70, 117.73, 112.29 ($^2J_{CF}$ = 21.37 Hz) 110.14; IR ($CHCl_3$): ν_{max} 3412, 3053, 2923, 2852, 1889, 1783, 1654, 1627, 1602, 1567, 1495, 1463, 1449, 1432, 1376, 1317, 1284, 1254, 1242, 1174, 1148, 1118, 1093, 1064, 1019 cm^{-1}; ESI-MS: *m/z* 325 $[M+H]^+$; HR-ESIMS: *m/z* 325.0540 calcd for $C_{18}H_{11}ClFN_2O + H^+$ (325.0538).

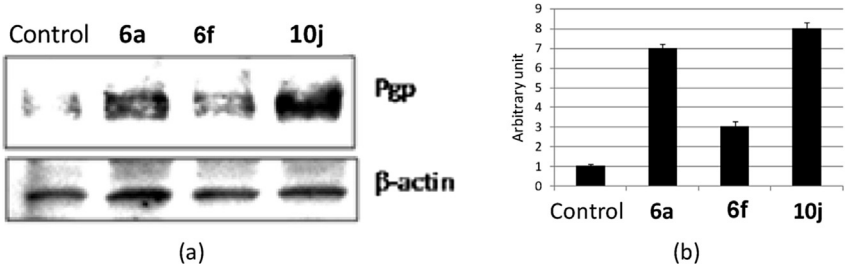

Fig. 3. The effect of fascaplysin **6a** and its analogs **6f**, **10j** on P-gp expression in LS-180 cells at 1 μM. (a) Western-blot (b) quantitation results of P-gp expression.

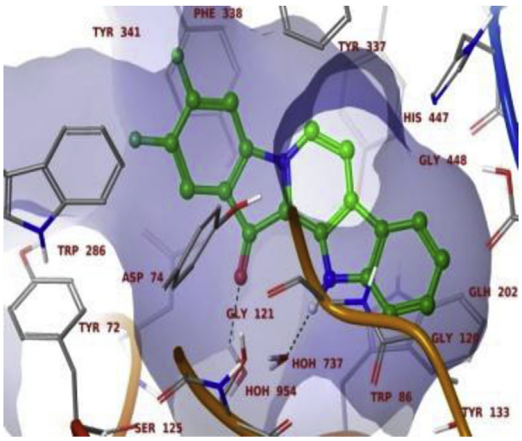

Fig. 4. Interaction of compound **6f** with the active site of AChE.

Table 3
Solubility of selected compounds **6a**, **6f** and **10j**.

Entry	Solubility (μg/ml)[a,b]			
	Water	PBS	SGF	SIF
6a	>1500	>1500	>1500	>1500
6f	>1500	80	80	<5
10j	800	800	800	800

[a] Thermodynamic experimental solubility.
[b] PBS, phosphate buffer saline; SGF, simulated gastric fluid; SIF, simulated intestinal fluid.

*4.3.6. (2-Chloro-4,5-difluorophenyl)(9H-pyrido[3,4-b]indol-1 yl) methanone (**9f**)*

Yellow solid; yield: 74%; m.p. 236–238 °C; HPLC: 90% (t_R = 14.70 min); ^{1}H NMR (400 MHz, DMSO-d$_6$, ppm): δ 12.28 (s, NH, 1H), 8.50–8.46 (m, 2H), 8.34 (d, *J* = 6.4 Hz, 1H), 7.94–7.84 (m, 3H), 7.64 (t, *J* = 6.0 Hz, 1H), 7.35 (t, *J* = 6.0 Hz, 1H); ^{19}F NMR (376.5 Hz, DMSO-d$_6$, ppm): δ −133.60 to −133.71 (m, 1F), −139.60 to −139.70 (m, 1F); ^{13}C NMR (100 MHz, DMSO-d$_6$, ppm): δ 193.70, 149.91 ($^1J_{CF}$ = 233.41 Hz), 148.10 ($^1J_{CF}$ = 247.74 Hz), 141.93, 137.94, 136.20, 135.27, 134.74, 131.39, 129.27, 125.93, 121.97, 120.58, 120.01, 119.86, 118.87, 118.57, 113.10; IR (KBr): ν_{max} 3423, 3059, 2922, 2850, 1900, 1794, 1646, 1628, 1592, 1565, 1463, 1452, 1430, 1378, 1339, 1317, 1286, 1248, 1208, 1062 cm^{-1}; ESI-MS: *m/z* 343 [M+H]$^+$; HR-ESIMS: *m/z* 343.0438 calcd for $C_{18}H_{10}ClF_2N_2O + H^+$ (343.0444).

*4.3.7. (2,5-Dichlorophenyl)(9H-pyrido[3,4-b]indol-1-yl)methanone (**9g**)*

Yellow solid; yield: 80%; m.p. 210–212 °C; HPLC: 92% (t_R = 12.97 min); ^{1}H NMR (400 MHz, CDCl$_3$, ppm): δ 10.32 (s, NH, 1H), 8.56 (d, *J* = 4.0 Hz, 1H), 8.20–8.18 (dd, *J* = 4.0, 8.0 Hz, 2H), 7.65–7.56 (m, 3H), 7.43–7.38 (m, 3H); ^{13}C NMR (100 MHz, CDCl$_3$, ppm): δ 196.08, 141.21, 139.70, 138.97, 136.85, 134.95, 132.55, 132.0, 131.68, 131.14, 131.10, 130.15, 129.72, 129.64, 121.99, 121.19, 119.47, 112.12; IR (CHCl$_3$): ν_{max} 3416, 3069, 3086, 3054, 3040, 2955, 2924, 2853, 2614, 2094, 1941, 1914, 1898, 1784, 1651, 1625, 1595, 1509, 1493, 1453, 1430, 1393, 1315, 1283, 1270, 1256, 1246, 1210, 1149, 1121, 1099, 1063, 1010 cm^{-1}; ESI-MS: *m/z* 341.06 [M+H]$^+$; HR-ESIMS: *m/z* 341.0206 calcd for $C_{18}H_{11}Cl_2N_2O + H^+$ (341.0242).

*4.3.8. Phenyl (9H-pyrido[3,4-b]indol-1-yl)methanone (**9h**)*

Yellow solid; yield 80%; m.p. 180–182 °C; HPLC: >99% (t_R = 17.11 min); ^{1}H NMR (400 MHz, CDCl$_3$, ppm): δ 10.45 (s, NH, 1H), 8.63–8.61 (m, 1H), 8.32 (d, *J* = 8.0 Hz, 2H), 8.20–8.17 (m, 2H), 7.63–7.52 (m, 5H), 7.37–7.35 (m, 1H); ^{13}C NMR (100 MHz, CDCl$_3$, ppm): δ 195.56, 141.04, 138.07, 137.59, 137.34, 136.29, 132.42, 131.68, 131.25, 129.30, 128.07, 121.83, 120.85, 120.78, 118.54, 112.03; IR (CHCl$_3$): ν_{max} 3430, 3378, 3055, 2922, 2850, 1899, 1640, 1619, 1596, 1574, 1492, 1464, 1426, 1373, 1317, 1247, 1212, 1149, 1118, 1087, 1060, 1013 cm^{-1}; ESI-MS: *m/z* 273.10 [M+H]$^+$; HR-ESIMS: *m/z* 273.1015 calcd for $C_{18}H_{13}N_2O + H^+$ (273.1022).

*4.3.9. (1H-indol-3yl)(9H-pyrido[3,4-b]indol-1-yl)methanone (**9i**)*

Yellow solid; yield: 65%; m.p. 220–222 °C; HPLC: 91% (t_R = 16.83 min); ^{1}H NMR (400 MHz, CDCl$_3$, ppm): δ 10.75 (s, NH, 1H), 9.45 (d, *J* = 4.0 Hz, 1H), 8.71 (s, NH, 1H), 8.70 (s, 1H), 8.57 (d, *J* = 8.0 Hz, 1H), 8.18–8.14 (m, 2H), 7.60 (d, *J* = 4.0 Hz, 2H), 7.48 (d, *J* = 8.0 Hz, 1H), 7.39–7.35 (m, 3H); ^{13}C NMR (100 MHz, CDCl$_3$ ppm): δ 187.33, 141.56, 138.43, 137.87, 137.81, 136.97, 135.92, 135.00, 130.72, 128.64, 127.18, 122.88, 122.04, 121.65, 120.02, 119.78, 117.93, 114.21, 112.98, 112.31; IR (CHCl$_3$): ν_{max} 3452, 3413, 3248, 3148, 3055, 2926, 2853, 2564, 2351, 2069, 1892, 1851, 1778, 1633, 1597, 1554, 1507, 1490, 1467, 1442, 1423, 1385, 1352, 1317, 1249, 1216, 1193, 1135, 1052, 1013 cm^{-1}; ESI-MS: *m/z* 312 [M+H]$^+$; HR-ESIMS: *m/z* 312.1132 calcd for $C_{20}H_{14}N_3O + H^+$ (312.1131).

*4.3.10. (2-Bromophenyl)(9H-pyrido[3,4-b]indol-1-yl)methanone (**9j**)*

Yellow solid; yield: 65%; m.p. 204–206 °C; HPLC: >99% (t_R = 14.97 min); ^{1}H NMR (400 MHz, CDCl$_3$, ppm): δ 10.48 (s, NH, 1H), 8.57 (d, *J* = 4.0 Hz, 1H), 8.18 (t, *J* = 4.0 Hz, 2H), 7.70–7.56 (m, 4H), 7.49–7.26 (m, 3H); ^{13}C NMR (100 MHz, CDCl$_3$, ppm): δ 198.28, 141.25, 140.33, 138.85, 136.93, 135.13, 133.17, 131.94, 131.32, 129.85, 129.57, 126.95, 121.98, 121.08, 120.71, 120.12, 119.28, 112.15; IR (CHCl$_3$): ν_{max} 3424, 3057, 2922, 2851, 2611, 1900, 1715, 1653, 1624, 1591, 1564, 1493, 1462, 1429, 1378, 1316, 1283, 1263, 1248, 1213, 1161, 1149, 1094, 1043, 1012 cm^{-1}; ESI-MS: *m/z* 351.01 [M+H]$^+$; HR-ESIMS: *m/z* 351.0124 calcd for $C_{18}H_{12}BrN_2O + H^+$ (351.0127).

*4.3.11. (2-Fluorophenyl)(9H-pyrido[3,4-b]indol-1-yl)methanone (**9k**)*

Yellow solid; yield: 70%; m.p. 198–200 °C; HPLC: 90% (t_R = 14.72 min); ^{1}H NMR (400 MHz, CDCl$_3$, ppm): δ 10.44 (s, NH, 1H), 8.57 (d, *J* = 4.0 Hz, 1H), 8.16 (t, *J* = 4.0 Hz, 2H), 7.79–7.76 (m, 1H), 7.62–7.53 (m, 3H), 7.37–7.19 (m, 3H); ^{19}F NMR (376.5 Hz, CDCl$_3$, ppm): δ −111.34 to −111.40 (m, 1F); ^{13}C NMR (100 MHz, CDCl$_3$, ppm): δ 195.58, 160.50 ($^1J_{CF}$ = 252.77 Hz), 141.15, 138.70, 136.72, 135.74, 133.02, 131.19, 131.17, 129.45, 123.89, 121.92, 120.98, 120.74, 119.16, 116.33, 112.09; IR (CHCl$_3$): ν_{max} 3398, 3051, 2923, 2852, 1649, 1629, 1612, 1596, 1579, 1566, 1494, 1463, 1448, 1428, 1378, 1338, 1282, 1264, 1246, 1147, 1118, 1102, 1085, 1061, 1020 cm^{-1}; ESI-MS: *m/z* 291.09 [M+H]$^+$; HR-ESIMS: *m/z* 291.0926 calcd for $C_{18}H_{12}FN_2O + H^+$ (291.0928).

*4.3.12. (4-Trifluoromethylphenyl)(9H-pyrido[3,4-b]indol-1-yl) methanone (**9l**)*

Yellow solid; yield: 75%; m.p. 201–203 °C; HPLC: >99% (t_R = 36.47 min); ^{1}H NMR (400 MHz, CDCl$_3$, ppm): δ 8.50 (d, *J* = 4.0 Hz, 1H), 8.37–8.26 (m, 4H), 7.86 (d, *J* = 8.0 Hz, 2H), 7.75 (d, *J* = 8.0 Hz, 1H), 7.61 (t, *J* = 8.0 Hz, 1H), 7.35 (t, *J* = 8.0 Hz, 1H); ^{19}F NMR (376.5 Hz, CDCl$_3$, ppm): δ −63.03 (s, 3F); ^{13}C NMR (100 MHz, CDCl$_3$, ppm): δ 194.57, 141.08, 140.56, 138.24, 137.38, 135.52, 133.60, 133.34, 131.95, 130.38, 129.54, 124.99, 124.96, 122.77, 121.92, 121.04, 120.75, 119.04, 112.08; IR (CHCl$_3$): ν_{max} 3393, 3066, 2922, 2852, 2675, 1904, 1696, 1649, 1626, 1598, 1578, 1514, 1494, 1428, 1404, 1328, 1317, 1249, 1217, 1167, 1067 cm^{-1}; ESI-MS: *m/z* 341.09 [M+H]$^+$; HR-ESIMS: *m/z* 341.0894 calcd for $C_{19}H_{12}F_3N_2O + H^+$ (341.0896).

*4.3.13. (2,4-Dimethoxyphenyl)(9H-pyrido[3,4-b]indol-1yl) methanone (**9m**)*

Yellow solid; yield: 66%; m.p. 233–235 °C; HPLC: 93% (t_R = 7.26 min); ^{1}H NMR (400 MHz, $CDCl_3$, ppm): δ 10.40 (s, NH, 1H), 8.54 (d, *J* = 4.0 Hz, 1H), 8.18–8.11 (m, 2H), 7.69–7.60 (m, 3H), 7.36–7.26 (m, 1H), 6.63–6.59 (m, 2H); 3.89 (s, 3H), 3.78 (s, 3H); ^{13}C NMR (100 MHz, $CDCl_3$, ppm): δ 196.86, 163.44, 160.30, 141.11, 138.27, 137.05, 136.72, 133.01, 31.47, 129.15, 121.79, 120.85, 120.63, 118.28, 111.98, 101.48, 99.26, 55.82, 55.52; IR (KBr): ν_{max} 3368, 3056, 30,003, 2925, 2850, 1731, 1644, 1623, 1577, 1503, 1493, 1463, 1427, 1315, 1282, 1160, 1131, 1087, 1062, 1030 cm^{-1}; ESI-MS: *m/z* 333 $[M+H]^+$; HR-ESIMS: *m/z* 333.1232 calcd for $C_{20}H_{17}N_2O_3$ + H^+ (333.1233).

*4.4. General procedure for synthesis of fascaplysin analogs **6a–g***

The β-carbolines **9a–g** (0.163 mmol) were heated at 220 °C for 15 min. The reaction was cooled and the product was recrystallized from CH_2Cl_2/diethyl ether producing corresponding quaternary fascaplysin analogs **6a–g** in 70–80% yield.

*4.4.1. Fascaplysin (**6a**)*

Brick red solid; yield: 80%; m.p. 230–232 °C; HPLC: 96% (t_R = 9.96 min); ^{1}H NMR (500 MHz, CD_3OD, ppm): δ 9.40 (d, *J* = 5.6 Hz, 1H), 8.98 (d, *J* = 5.8 Hz, 1H), 8.48 (d, *J* = 7.9 Hz, 1H), 8.35 (d, *J* = 8.0 Hz,1H), 8.08 (d, *J* = 7.3 Hz, 1H), 7.96 (t, *J* = 7.7 Hz, 1H), 7.89 (t, *J* = 7.7 Hz, 1H), 7.79 (d, *J* = 8.3 Hz, 1H), 7.73 (t, *J* = 7.4 Hz, 1H), 7.54 (t, *J* = 7.4 Hz, 1H); ^{13}C NMR (100 MHz, CD_3OD, ppm): δ 183.25, 148.89, 148.75, 142.92, 138.32, 135.91, 133.12, 132.75, 127.59, 126.85, 125.57, 125.23, 124.66, 123.62, 121.26, 121.19, 116.49, 114.68; IR ($CHCl_3$): ν_{max} 3368, 2923, 2359, 1621, 1506, 1046 cm^{-1}; ESI-MS: *m/z* 271.09 $[M-Cl]^+$; HR-ESIMS: *m/z* 271.0843 calcd for $C_{18}H_{11}N_2O^+$ (271.0866).

*4.4.2. 4-Chloro fascaplysin (**6b**)*

Brick red solid; yield: 75%; m.p. 234–236 °C; HPLC: 97% (t_R = 5.05 min); ^{1}H NMR (400 MHz, CD_3OD, ppm): δ 9.27 (d, *J* = 6.4 Hz, 1H), 8.88 (d, *J* = 6.0 Hz, 1H), 8.45–8.39 (m, 2H), 7.94 (d, *J* = 8.0 Hz, 1H), 7.84–7.80 (m, 1H), 7.74–7.68 (m, 2H),7.46 (t, *J* = 6.8 Hz, 1H); ^{13}C NMR (100 MHz, CD_3OD, ppm): δ 182.0, 149.73, 149.08, 143.25, 136.18, 133.02, 132.99, 132.74, 127.90, 127.77, 125.37, 124.74, 124.24, 121.26, 121.09, 117.68, 11,470; IR (KBr): ν_{max} 3468, 2925, 1637, 1418, 1021 cm^{-1}; ESI-MS: *m/z* 305 $[M-Cl]^+$; HR-ESIMS: *m/z* 305.0475 calcd for $C_{18}H_{10}ClN_2O^+$ (305.0476).

*4.4.3. 4-Chloro-5-fluoro fascaplysin (**6c**)*

Brick red solid; yield: 70%; m.p. 218–220 °C; HPLC: 95% (t_R = 6.68 min); ^{1}H NMR (400 MHz, CD_3OD, ppm): δ 9.25 (d, *J* = 4.0 Hz, 1H), 8.88 (d, *J* = 6.0 Hz, 1H), 8.60 (d, *J* = 5.2 Hz, 1H), 8.39 (d, *J* = 7.6 Hz, 1H), 7.90 (d, *J* = 6.8 Hz, 1H), 7.83–7.70 (m, 2H), 77.45 (t, *J* = 7.6 Hz, 1H); ^{19}F NMR (376.5 Hz, CD_3OD, ppm): δ −111.29 to −111.32 (m, 1F); ^{13}C NMR (100 MHz, CD_3OD, ppm): δ 181.24, 161.03 ($^1J_{CF}$ = 255.29 Hz), 149.04, 143.87 ($^2J_{CF}$ = 213.79 Hz), 136.25, 136.02, 133.16, 130.85, 128.10, 128.02, 127.84, 125.43, 124.84, 123.98, 121.26, 119.84, 114.73, 114.54; IR (KBr): ν_{max} 3459, 2925, 1619, 1469,1048 cm^{-1}; ESI-MS: *m/z* 323 $[M-Cl]^+$; HR-ESIMS: *m/z* 323.0379 calcd for $C_{18}H_9ClFN_2O^+$ (323.0382).

*4.4.4. 3,4-Dichloro fascaplysin (**6d**)*

Brick red solid; yield: 72%; m.p. 243–245 °C; HPLC: 98% (t_R = 7.90 min); ^{1}H NMR (400 MHz, CD_3OD, ppm): δ 10.04 (s, 1H), 8.86 (d, *J* = 8.0 Hz, 1H), 8.41 (d, *J* = 8.0 Hz, 1H), 7.95–7.81 (m, 3H), 7.74–7.72 (m, 1H), 7.46 (t, *J* = 8.0 Hz, 1H); ^{13}C NMR (100 MHz, CD_3OD, ppm): δ 181.38, 149.64, 145.78, 145.17, 144.76, 144.30, 136.73, 134.28, 130.90, 127.06, 125.67, 125.51, 124.97, 123.92, 123.67, 121.88, 120.81, 114.83; IR (KBr): ν_{max} 3453, 2924, 1637, 1508, 1070 cm^{-1}; ESI-MS: *m/z* 339 $[M-Cl]^+$; HR-ESIMS: *m/z* 339.0093 calcd for $C_{18}H_9Cl_2N_2O^+$ (339.0086).

*4.4.5. 6-Chloro fascaplysin (**6e**)*

Brick red solid; yield: 74%; m.p. 231–233 °C; HPLC: 93% (t_R = 5.39 min); ^{1}H NMR (400 MHz, CD_3OD, ppm): δ 9.27 (d, *J* = 6.0 Hz, 1H), 8.85 (d, *J* = 6.0 Hz, 1H), 8.36 (d, *J* = 8.0 Hz, 1H), 8.19 (d, *J* = 8.0 Hz, 1H), 7.82–7.74 (m, 2H), 7.71–7.69 (m, 1H), 7.60 (d, *J* = 8.0 Hz, 1H), 7.42 (t, *J* = 7.6 Hz, 1H); ^{13}C NMR (100 MHz, CD_3OD, ppm): δ 180.46, 149.74, 149.0, 138.71, 136.06, 135.04, 133.99, 130.21, 127.48, 126.92, 125.27, 124.71, 124.43, 123.39, 122.47, 121.10, 115.20, 114.70; IR (KBr): ν_{max} 3460, 2925, 1637, 1510, 1020 cm^{-1}; ESI-MS: *m/z* 305.0 $[M-F]^+$; HR-ESIMS: *m/z* 305.0480 calcd for $C_{18}H_{10}ClN_2O^+$ (305.0476).

*4.4.6. 4,5-Difluoro fascaplysin (**6f**)*

Brick red solid; yield: 75%; m.p. 240–242 °C; HPLC: 92% (t_R = 5.68 min); ^{1}H NMR (400 MHz, CD_3OD, ppm): δ 9.18 (d, *J* = 6.4 Hz, 1H), 8.82 (d, *J* = 6.4 Hz, 1H), 8.54 (d, *J* = 6.4 Hz, 1H), 8.33 (d, *J* = 8.0 Hz, 1H), 7.83 (d, *J* = 6.8 Hz, 1H), 7.76–7.73 (m, 1H), 7.66–7.64 (m, 1H), 7.40–7.35 (m,1H); ^{19}F NMR (376.5 Hz, DMSO-d_6, ppm): δ −134.60 to −134.71 (m, 1F), −140.60 to −140.70 (m, 1F); ^{13}C NMR (100 MHz, CD_3OD, ppm): δ 181.1, 161.21 ($^1J_{CF}$ = 255.05 Hz), 149.22, 144.05 ($^2J_{CF}$ = 213.54 Hz), 136.43, 133.33, 131.02, 128.27, 128.02, 125.60, 125.49, 124.91, 124.16, 121.44, 120.01, 18.87, 114.91, 114.71; IR (KBr): ν_{max} 3467, 2825, 1638, 1509, 1087 cm^{-1}; ESI-MS: *m/z* 307 $[M-Cl]^+$; HR-ESIMS: *m/z* 307.0679 calcd for $C_{18}H_9F_2N_2O^+$ (307.0677).

*4.4.7. 5-Chloro fascaplysin (**6g**)*

Brick red solid; yield: 80%; m.p. 236–238 °C; HPLC: 97% (t_R = 4.80 min); ^{1}H NMR (400 MHz, CD_3OD, ppm): δ 9.27 (d, *J* = 5.6 Hz, 1H), 8.88 (d, *J* = 5.6 Hz, 1H), 8.44–8.39 (m, 2H), 7.94 (d, *J* = 8.0 Hz, 1H), 7.83–7.67 (m, 3H), 7.45 (t, *J* = 7.2 Hz, 1H); ^{13}C NMR (100 MHz, CD_3OD, ppm): δ 181.93, 149.65, 149.04, 144.24, 143.23, 136.12, 132.67, 127.78, 127.70, 125.26, 124.68, 124.16, 121.20, 120.97, 117.55, 114.64; IR (KBr): ν_{max} 3468, 2964, 1637, 1417, 1020 cm^{-1}; ESI-MS: *m/z* 305 $[M-Cl]^+$; HR-ESIMS: *m/z* 305.0478 calcd for $C_{18}H_{10}ClN_2O^+$ (305.0476).

*4.5. General procedure for synthesis of β-carbolinium analogs **10a** and **10h–l***

The mixture of β-carbolines **9a** and **9h–m** (0.1 g, 1 mmol), methyl iodide (1.5 mmol) and 5 mL ACN was heated for 12 h at 80 °C in sealed tube. The mixture was allowed to cool at 25 °C. The obtained products were recrystallized with dichloromethane to get corresponding D-ring opened β-carbolinium analogs **10a** and **10h–l** in 60–75% yield.

*4.5.1. 1-(2-Chloro-benzoyl)-2-methyl beta-carbolinium iodide (**10a**)*

Yellow solid; yield: 60%; m.p. 220–222 °C; HPLC: 97% (t_R = 31.23 min); ^{1}H NMR (400 MHz, CD_3OD, ppm): δ 8.74 (d, *J* = 6.4 Hz, 1H), 8.57 (d, *J* = 6.4 Hz, 1H), 8.38 (d, *J* = 8.0 Hz, 1H), 7.98 (d, *J* = 8.0 Hz, 1H), 7.76–7.69 (m, 2H), 7.61–7.53 (m, 3H), 7.43 (t, *J* = 7.6 Hz, 1H), 4.24 (s, 3H); ^{13}C NMR (100 MHz, CD_3OD, ppm): δ 167.73, 145.98, 136.76, 134.44, 134.23, 133.94, 133.53, 132.28, 132.0, 131.69, 128.02, 124.35, 123.22, 120.89, 118.71, 113.92, 54.85; IR (KBr): ν_{max} 3459, 2925, 1630, 1586, 1226, 1042 cm^{-1}; ESI-MS: *m/z* 321 $[M-I]^+$; HR-ESIMS: *m/z* 321.0787 calcd for $C_{19}H_{14}ClN_2O^+$ (321.0789).

*4.5.2. 1-Benzoyl-2-methyl beta-carbolinium iodide (**10h**)*

Yield solid; yield: 68%; m.p. 233–235 °C; HPLC: 99% (t_R = 26.34 min); ^{1}H NMR (400 MHz, CD_3OD, ppm): δ 8.74 (d, *J* = 6.4 Hz, 1H), 8.61 (d, *J* = 6.4 Hz, 1H), 8.40 (d, *J* = 8.0 Hz, 1H), 7.92–7.90 (m, 2H), 7.77–7.71 (m, 2H), 7.59–7.54 (m, 3H), 7.42 (t, *J* = 7.2 Hz, 1H), 4.25 (s, 3H), 3.11 (s, 3H); ^{13}C NMR (100 MHz, CD_3OD, ppm): δ 188.49, 146.78, 137.93, 136.77, 136.1, 135.74, 134.89, 134.32, 131.79, 131.14, 124.65, 123.74, 120.80, 119.41, 114.01, 46.61; IR (KBr): ν_{max} 3467, 2985, 2063, 1671, 1593, 1201, 1019 cm^{-1}; ESI-MS: *m/z* 287 $[M-I]^+$; HR-ESIMS: *m/z* 287.1177 calcd for $C_{19}H_{15}N_2O^+$ (287.1178).

*4.5.3. 1-(3-Indoloyl)-2-methyl beta-carbolinium iodide (**10i**)*

Yellow solid; yield: 62%; m.p. 240–242 °C; HPLC: >99% (t_R = 18.30 min); ^{1}H NMR (400 MHz, DMSO-d_6, ppm): δ 8.96 (d, *J* = 6.4 Hz, 1H), 8.87 (d, *J* = 8.0 Hz, 1H), 8.58 (d, *J* = 8.0 Hz, 1H), 8.42 (s, 1H), 8.17 (s, 1H), 7.80 (t, *J* = 8.0 Hz, 1H), 7.66–7.63 (m, 2H), 7.52–7.43 (m. 3H), 4.37 (s, 3H); ^{13}C NMR (100 MHz, DMSO-d_6, ppm): δ 178.33, 144.68, 140.86, 137.62, 136.34, 136.30, 135.03, 134.47, 133.04, 132.37, 125.20, 124.57, 123.63, 123.49, 121.84, 121.53, 119.19, 117.84, 115.92, 113.05, 40.02; IR (KBr): ν_{max} 3467, 3419, 2930, 2855, 2427, 1634, 1618, 1584, 1457, 1248, 882 cm^{-1}; ESI-MS: *m/z* 326 $[M-I]^+$; HR-ESIMS: *m/z* 326.1287 calcd for $C_{21}H_{16}N_3O^+$ (326.1287).

*4.5.4. 1-(2-Bromo-benzoyl)-2-methyl beta-carbolinium iodide (**10j**)*

Yellow solid; yield: 70%; m.p. 242–244 °C; HPLC: 99% (t_R = 36.33 min); ^{1}H NMR (400 MHz, CD_3OD, ppm): δ 8.75 (d, *J* = 6.4 Hz, 1H), 8.58 (d, *J* = 6.4 Hz, 1H), 8.39 (d, *J* = 8.0 Hz, 1H), 7.95 (d, *J* = 4.8 Hz, 1H), 7.76–7.73 (m, 2H), 7.62–7.59 (m, 3H), 7.43 (t, *J* = 7.6 Hz, 1H), 4.21 (s, 3H); ^{13}C NMR (100 MHz, CD_3OD, ppm): δ 188.49, 146.78, 137.93, 136.77, 136.61, 136.35, 136.10, 135.74, 134.89, 134.32, 131.79, 131.14, 124.65, 123.74, 120.80, 119.41, 114.01, 46.61; IR (KBr): ν_{max} 3467, 2926, 2057, 1628, 1581, 1226, 1034 cm^{-1}; ESI-MS: *m/z* 365 $[M-I]^+$; HR-ESIMS: *m/z* 365.0284 calcd for $C_{19}H_{14}BrN_2O^+$ (365.0284).

*4.5.5. 1-(2-Fluoro-benzoyl)-2-methyl beta-carbolinium iodide (**10k**)*

Yellow solid; yield: 65%; m.p. 234–236 °C; HPLC: >99% (t_R = 29.61 min); ^{1}H NMR (400 MHz, CD_3OD, ppm): δ 8.77 (d, *J* = 6.4 Hz, 1H), 8.60 (d, *J* = 6.4 Hz, 1H), 8.40 (d, *J* = 8.0 Hz, 1H), 7.97–7.95 (m, 1H), 7.78–7.76 (m, 2H), 7.64–7.62 (m, 3H), 7.46 (t, *J* = 7.2 Hz, 1H), 4.23 (s, 3H); ^{19}F NMR (376.5 Hz, DMSO-d_6, ppm): δ −124.25 to −124.32 (m, 1F); ^{13}C NMR (100 MHz, CD_3OD, ppm): δ 184.66, 164.57, 163.13, 151.62, 146.79, 142.06, 140.48, 140.40, 136.16, 134.43, 133.28, 127.23, 124.60, 120.82, 119.43, 118.73, 118.56, 114.06, 46.46; IR (KBr): ν_{max} 3759, 3453, 2956, 2924, 2073, 1747, 1673, 1605, 1632, 1520, 1482, 1452, 1333, 1316, 1272, 1163, 1150, 1116, 1019 cm^{-1}; ESI-MS: *m/z* 305 $[M-I]^+$; HR-ESIMS: *m/z* 305.1083 calcd for $C_{19}H_{14}FN_2O^+$ (305.1084).

*4.5.6. 1-(4-Trifluromethyl-benzoyl)-2-methylbeta-carbolinium iodide (**10l**)*

Yellow solid; yield: 75%; m.p. 236–238 °C; HPLC: >99% (t_R = 14.72 min); ^{1}H NMR (400 MHz, CD_3OD, ppm): δ 8.78 (d, *J* = 6.4 Hz, 1H), 8.65 (d, *J* = 6.4 Hz, 1H), 8.41 (d, *J* = 8.0 Hz, 1H), 8.11 (d, *J* = 8.0 Hz, 2H), 7.89 (d, *J* = 4.2 Hz, 2H), 7.76–7.72 (m, 1H), 7.55 (d, *J* = 8.4 Hz, 1H), 7.45–7.41 (m, 1H), 7.28–7.23 (m, 1H), 4.27 (s, 3H); ^{19}F NMR (376.5 Hz, DMSO-d_6, ppm): δ −61.89 (s, 3F); ^{13}C NMR (100 MHz, CD_3OD, ppm): δ 167.19, 145.99, 136.77, 134.98, 134.46, 134.36, 133.54, 131.19, 126.64, 126.61, 124.34, 123.23, 120.89, 118.71, 113.92, 48.51; IR (KBr): ν_{max} 3453, 2956, 2073, 1632, 1520, 1163 cm^{-1}; ESI-MS: *m/z* 355 $[M-I]^+$; HR-ESIMS: *m/z* 355.1042 calcd for $C_{20}H_{14}F_3N_2O^+$ (355.1052).

*4.6. General procedure for synthesis N-acyl β-carbolines 13a–n and N-alkylated β-carbolines **15a–h***

The synthesis of *N*-acyl β-carbolines **13a–n** and *N*-alkylated β-carbolines **15a–h** and their spectral data has been described in our earlier paper [24].

4.7. Cell culture and treatments

Human colorectal adenocarcinoma LS-180 cells were purchased from ECACC, England. Normal Human gingival fibroblast (hGF) cell line was a gift from Dr. Anil Ballapure, CDRI, Lucknow, India. Cells were grown in MEM growth medium mixed in the ratio of 1: 1. The media for the cell lines were supplemented with 1% MEM non-essential amino acids along with 10% FCS, 100 U penicillin G and 100 μg/ml of streptomycin. Cells were grown in 5% CO_2 at 37 °C with 95% humidity. All the test compounds were dissolved in DMSO for treatment of LS-180 cells, while the untreated control cultures received only the vehicle (DMSO < 0.2%).

4.8. P-gp induction assay

All synthesized compounds were screened for their ability to induce P-gp using the rhodamine 123 (Rh123) cell exclusion method. In this method, the P-gp function was evaluated in terms of rhodamine 123 (Rh123) accumulation and efflux [26]. Briefly, the protocol used is as follows: colorectal LS-180 cells were seeded at a density of 2 × 104 per well of a 96-well plate and were allowed to grow for the next 24 h. Cells were further incubated with the test compounds to a final concentration of 1 μM and rifampicin (positive control) to a final concentration of 10 μM in complete media for 48 h. The final concentration of DMSO was kept at 0.1%. The drugs were removed and cells were incubated with HANKS buffer for 40 min before further incubation with HANKS buffer (containing 10 μM of Rh123 as a Pgp substrate) for 90 min. At the end of Rh123 treatment cells were washed four times with cold PBS followed by cell lysis for 1 h using 200 μl of lysis buffer (0.1% Triton X-100 and 0.2 N NaOH). A total of 100 μl of lysate was used for reading fluorescence of Rh123 at 485/529 nm. Samples were normalized by dividing fluorescence of each sample with total protein present in the lysate.

4.9. Cell viability assay

The cell proliferation assay was performed in human colorectal adenocarcinoma LS-180 cells and normal human gingival fibroblast (hGF) cells. Cells (1×10^4) were seeded into each well of the 96-well microplate for 24 h. Cells were treated with 10 μM of each compound for 24 h. The MTT dye was then added to each well 4 h prior to the termination of experiment. Formazan crystals were dissolved in DMSO before recording absorbance at 570 nm. Cell viability of the untreated control sample was considered to be 100%, while viability of test samples was calculated using the following formula:

$$\%\ \text{Cell viability} = \frac{\text{OD(test)}}{\text{OD(control)}} \times 100$$

4.10. In vitro AChE inhibition assay

Acetylcholinesterase (AChE, E.C. 3.1.1.7, from electric eel, Type V-S, 827 U/mg solid; 1256 U/mg of protein), 5,5'-dithiobis-(2-nitrobenzoic acid) (Ellman's reagent, DTNB), acetylthiocholine

iodide (ATChI) and donepezil were purchased from Sigma–Aldrich. Compounds were dissolved in water to make 10 mM stock solution. Desired concentrations in the range of 1–100 μM were prepared by further dilutions with PBS. All assays were carried out in 96-well plate in 0.1 M NaH_2PO_4/Na_2HPO_4 buffer, pH 7.2, using Biotage Microplate Reader. AChE stock solution (1 mg/mL in 0.1 M sodium phosphate buffer, pH 7.2) was diluted to produce 5 μg/ml working solution for enzyme inhibition studies. Each well of 96-well plate consisted of total 200 μL assay medium, comprising 16 μL of enzyme solution, 4 μL of vehicle (PBS 7.2, control) or test compound, 154 μL of phosphate buffer (pH 7.2), 6 μL of 10 mM DTNB (final concentration of DTNB, 0.3 mM) and 20 μl of 10 mM ATChI (final concentration of ATChI, 1 mM). Initially, test compounds (along with a parallel PBS 7.2 as a control) were pre-incubated at 37 °C with the enzyme for 30 min followed by the addition of DTNB, ATChI and PBS (pH 7.2) to make up the volume. The activity was determined by measuring the increase in absorbance at 412 nm after different time intervals at 37 °C. Percent inhibition values were calculated from the slopes of absorbance readings *versus* different time intervals for control and test compounds. Each concentration was assayed in triplicate [27].

4.11. Determination of aqueous solubility by 96-well plate-based assay

This was determined in water, PBS, SGF, and SIF as described earlier [28].

4.12. Molecular modeling of the fascaplysin analogs with human AChE

Docking studies were performed using Glide module of Schrodinger Software implemented in the Maestro modeling package (Schrodinger, Inc., LLC, NewYork, USA) using default settings. The E2020 (Donepezil) bound to Human AChE (PDB: 4EY7; resolution, 2.35 A^0) was used in docking studies. Briefly, human AChE was imported from protein data bank [29] and prepared using Protein preparation wizard for H-bond optimization, heterogeneous state generation, protonation and overall minimization. Grid file of docking was constructed considering the bound ligand donepezil as centroid of the ligand and binding site of 20 A^0 radius box. All ligands were sketched in maestro, prepared using Ligprep and docked by Glide molecular docking software in XP mode.

4.13. Statistical analysis

Data are expressed as mean ± SD of three independent experiments unless otherwise indicated. The comparisons were made between control and treated groups or the entire intra-group using the Bonferroni test through the Instat-2 software. p values $^*<0.05$ were considered significant. p value $^*<0.05$, $^{**}<0.01$, $^{***}<0.001$.

Acknowledgments

SM and PJ are thankful to the CSIR for award of a Senior Research Fellowship. VK thanks UGC for the award of research fellowship. SSB is thankful to ICMR for Research Associateship. Authors thank analytical department, IIIM for NMR, MS and IR analysis of synthesized compounds. This work was supported by CSIR 12th FYP grant BSC-0205.

Appendix A. Supplementary data

Supporting information available. Spectral data scans. This material is available free of charge *via* the internet at http://sciencedirect.com.

Supplementary data related to this article can be found at http://dx.doi.org/10.1016/j.ejmech.2015.10.049.

References

[1] Y.J. Wang, H.D. Zhou, X.F. Zhou, Clearance of amyloid-beta in Alzheimer's disease: progress, problems and perspectives, Drug Discov. Today 11 (2006) 931–938.
[2] Alzheimers Association, Alzheimer's disease facts and figures, Alzheimers Dement. 8 (2012) 131–168, 11, (2015), 332–384.
[3] P. Tiraboschi, L.A. Hansen, L.J. Thal, J. Corey-Bloom, The importance of neuritic plaques and tangles to the development and evolution of AD, Neurology 62 (2004) 1984–1989.
[4] K.G. Mawuenyega, W. Sigurdson, V. Ovod, L. Munsell, T. Kasten, J.C. Morris, K.E. Yrasheski, R.J. Bateman, Decreased clearance of CNS β-amyloid in Alzheimer's disease, Science 330 (2010) 1774.
[5] D.M.E.v. Assema, M. Lubberink, M. Bauer, W.M.v.d. Flier, R.C. Schuit, A.D. Windhorst, E.F.I. Comans, N.J. Hoetjes, N. Tolboom, O. Langer, M. Muller, P. Scheltens, A.A. Lammertsma, B.N.M.v. Berckel, Blood–brain barrier P-glycoprotein function in Alzheimer's disease, Brain 135 (2012) 181–189.
[6] F.C. Lam, R. Liu, P. Lu, A.B. Shapiro, J.M. Renoir, F.J. Sharom, P.B. Reiner, β-Amyloid efflux mediated by P-glycoprotein, J. Neurochem. 76 (2001) 1121–1128.
[7] M.D. Perloff, E. Stormer, L.L. von Moltke, D.J. Greenblatt, Rapid assessment of P-glycoprotein inhibition and induction in vitro, Pharm. Res. 20 (2003) 1177–1183.
[8] R. Xie, L.H. Tan, E.C. Polasek, C. Hong, M. Teillol-Foo, T. Gordi, A. Sharma, D.J. Nickens, T. Arakawa, D.W. Knuth, E.J. Antal, CYP3A and P-glycoprotein activity induction with St. John's Wort in healthy volunteers from 6 ethnic populations, J. Clin. Pharmacol. 45 (2005) 352–356.
[9] R. Tian, N. Koyabu, S. Morimoto, Y. Shoyama, H. Ohtani, Y. Sawada, Functional induction and de-induction of P-glycoprotein by St. John's Wort and its ingredients in a human colon adenocarcinoma cell line, Drug Metab. Dispos. 33 (2005) 547–554.
[10] U.I. Schwarz, H. Hanso, R. Oertel, S. Miehlke, E. Kuhlisch, H. Glaeser, M. Hitzl, G.K. Dresser, R.B. Kim, W. Kirch, Induction of intestinal P-glycoprotein by St John's Wort reduces the oral bioavailability of talinolol, Clin. Pharmacol. Ther. 81 (2007) 669–678.
[11] M.D. Perloff, L.L. von Moltke, E. Stormer, R.I. Shader, D.J. Greenblatt, Saint John's Wort: an in vitro analysis of P-glycoprotein induction due to extended exposure, Br. J. Pharmacol. 134 (2001) 1601–1608.
[12] D.G. Teotico, J.J. Bischof, L. Peng, S.A. Kliewer, M.R. Redinbo, Structural basis of human pregnane X receptor activation by the hops constituent colupulone, Mol. Pharmacol. 74 (2008) 1512–1520.
[13] A.H. Abuznait, H. Qosa, B.A. Busnena, K.A. El Sayed, A. Kaddoumi, Olive-oil-derived oleocanthal enhances β-amyloid clearance as a potential neuroprotective mechanism against Alzheimer's disease: in vitro and in vivo studies, ACS Chem. Neurosci. 4 (2013) 973–982.
[14] J.B. Bharate, Y.S. Batarseh, A. Wani, S. Sharma, R.A. Vishwakarma, A. Kaddoumi, A. Kumar, S.B. Bharate, Synthesis and P-glycoprotein induction activity of colupulone analogs, Org. Biomol. Chem. 13 (2015) 5488–5496.
[15] J.B. Bharate, A. Wani, S. Sharma, S.I. Reja, M. Kumar, R.A. Vishwakarma, A. Kumar, S.B. Bharate, Synthesis, and the antioxidant, neuroprotective and P-glycoprotein induction activity of 4-arylquinoline-2-carboxylates, Org. Biomol. Chem. 12 (2014) 6267–6277.
[16] P. Joshi, S. Singh, A. Wani, S. Sharma, S.K. Jain, B. Singh, B.D. Gupta, N.K. Satti, S. Koul, I.A. Khan, A. Kumar, S.B. Bharate, R.A. Vishwakarma, Osthol and curcumin as inhibitors of human Pgp and multidrug efflux pumps of *Staphylococcus aureus*: reversing the resistance against frontline antibacterial drugs, Med. Chem. Commun. 5 (2014) 1540–1547.
[17] R. Mudududdla, S.K. Guru, A. Wani, S. Sharma, P. Joshi, R.A. Vishwakarma, A. Kumar, S. Bhushan, S.B. Bharate, 3-(Benzo[d][1,3]dioxol-5-ylamino)-N-(4-fluorophenyl)thiophene-2-carboxamide overcomes cancer chemoresistance via inhibition of angiogenesis and P-glycoprotein efflux pump activity, Org. Biomol. Chem. 13 (2015) 4296–4309.
[18] D.M. Roll, C.M. Ireland, Fascaplysin, an unusual antimicrobial pigment from the marine sponge *Fascaplysinopsis* sp. J. Org. Chem. 53 (1988) 3276–3278.
[19] L. Nathaniel, S.L. Segraves, T.A. Johnson, S.A. Said, X. Fu, F.J. Schmitz, H. Pietraszkiewicz, F.A. Valeriote, C. Phillip, Structures and cytotoxicities of fascaplysin and related alkaloids from two marine phyla-fascaplysinopsis sponges and didemnum tunicates, Tetrahedron Lett. 44 (2003) 3471–3475.
[20] R. Soni, L. Muller, P. Furet, J. Schoepfer, C. Stephan, S. Zumstein-Mecker, H. Fretz, B. Chaudhuri, Inhibition of cyclin-dependent kinase 4 (Cdk4) by fascaplysin, a marine natural product, Biochem. Biophys. Res. Commun. 275 (2000) 877–884.
[21] N.L. Segraves, S.J. Robinson, D. Garcia, S.A. Said, X. Fu, F.J. Schmitz, H. Pietraszkiewicz, F.A. Valeriote, P. Crews, Comparison of fascaplysin and related alkaloids: a study of structures, cytotoxicities, and sources, J. Nat. Prod. 67 (2004) 783–792.
[22] S.B. Bharate, S. Manda, N. Mupparapu, N. Battini, R.A. Vishwakarma, Chemistry and biology of fascaplysin, a potent marine-derived Cdk-4 inhibitor, Mini-Rev. Med. Chem. 12 (2012) 650–664.

[23] S.B. Bharate, S. Manda, P. Joshi, B. Singh, R.A. Vishwakarma, Total synthesis and anti-cholinesterase activity of marine derived bis-indole alkaloid fascaplysin, Med. Chem. Commun. 3 (2012) 1098–1103.
[24] S. Manda, S.I. Khan, S.K. Jain, S. Mohammed, B.L. Tekwani, I.A. Khan, R.A. Vishwakarma, S.B. Bharate, Synthesis, antileishmanial and antitrypanosomal activities of N-substituted tetrahydro-β-carbolines, Bioorg. Med. Chem. Lett. 24 (2014) 3247–3250.
[25] B. Qin, X. Liu, J. Shi, K. Zheng, H. Zhao, X. Feng, Enantioselective cyanosilylation of r,r-dialkoxy ketones catalyzed by proline-derived in-situ-prepared N-oxide as bifunctional organocatalyst, J. Org. Chem. 72 (2007) 2374–2378.
[26] M. Kageyama, K. Fukushima, T. Togawa, K. Fujimoto, M. Taki, A. Nishimura, Y. Ito, N. Sugioka, N. Shibata, K. Takada, Relationship between excretion clearance of rhodamine 123 and P-glycoprotein (P-gp) expression induced by representative P-gp inducers, Biol. Pharm. Bull. 4 (2006) 779–784.
[27] S.B. Bharate, L. Guo, T.E. Reeves, D.M. Cerasoli, C.M. Thompson, Bisquaternary pyridinium oximes: comparison of in vitro reactivation potency of compounds bearing aliphatic linkers and heteroaromatic linkers for paraoxon-inhibited electric eel and recombinant human acetylcholinesterase, Bioorg. Med. Chem. 18 (2010) 787–794.
[28] S.S. Bharate, R.A. Vishwakarma, Thermodynamic equilibrium solubility measurements in simulated fluids by 96-well plate method in early drug discovery, Bioorg. Med. Chem. Lett. 25 (2015) 1561–1567.
[29] C. Jonah, J.R. Michael, B. Fiana, S.C. Michael, N.G. Ebony, L. James, C.F. Matthew, J.H. Jude, Structures of human acetylcholinesterase in complex with pharmacologically important ligands, J. Med. Chem. 55 (2012) 10282–10286.